

## **An influence of the barrel toroid coil displacements on the intercoil sector magnetic field behaviour**

**V. I. Klioukhine, B. I. Klochkov**

IHEP, Protvino, Russia

### **Introduction**

In this note we estimate a behaviour of the ATLAS toroid magnetic field in dependence of one and two coil displacements using a 2-dimensional computer model of the toroid magnetic system simulated with the modified CERN POISSON program package [1]. For central part of the barrel toroid such an approximation is well enough to feel an order of magnitude of the field changes. The modifications done for the POISSON package permitted us to describe toroid magnetic system as full configuration of eight coils together with simple geometry used for the hadronic tile calorimeter including its support girder. A relative accuracy of these finite element calculations is around ten Gauss and meets the requirements on the barrel toroid field manifested in the ATLAS Technical Proposal [2].

### **Magnetic system description**

General layout of the barrel toroid magnetic system cross section used for the calculations is shown in Fig. 1. To describe such a system we utilize an equilateral triangle mesh consisting of 250 000 nodes with an average cell size of 5.2 cm changing from few millimetres in the most crucial regions to 10.5 cm outwards the coils. The geometry and electrical parameters of the system

correspond to that ones listed in [3]. To describe the magnetic properties of the tile calorimeter steel we use a B–H dependence table from [4]. A saturation of the girder steel caused by solenoidal field does not take into account in present studies.

The elements of magnetic system are as follows:

- 8 barrel coils are placed at the azimuthal angles of 22.5, 67.5, 112.5, 157.5, 202.5, 247.5, 292.5, and 337.5 degrees counterclockwise with respect to  $x$ -axis which is horizontal. Further we will pay much attention to the coils at 22.5 and 67.5 degrees and will call these coils as the ‘first’ coil and ‘second’ coil, accordingly. A toroid sector between 8 and 1 coils will be called as the ‘first’ sector, the same between 1 and 2 coils – as the ‘second’ sector.

The coils in cross section consist of two halves: an inner one with positive current density and an outer one with negative current density. The centre-of-gravity of the inner half is at the radius of 5.315 m, the same of the outer half is at the radius of 9.145 m. The middle of radial distance between those centres-of-gravity will be called ‘the coil centre’ and will be used to rotate the coil counterclockwise and clockwise with respect to this point. In all the coil transformations the radial distance between the coil halves assumes to be stringent and will not change.

Each coil half consists of two conductor pancakes having a radial thickness of 45 cm, azimuthal width of 15 cm and separated by 5 cm in azimuthal direction. A total Ampere-turns in each pancake is 1.52 MA which corresponds to the total operating current in the whole toroid of 24.32 MA-turns.

- The girder of hadronic tile calorimeter is described as two steel tubes: one with an inner radius of 3.78 and an outer radius of 3.92 m and another one with an inner radius of 4.1 and an outer radius of 4.2 m. A space between these tubes is filled with an iron with a stacking factor of 0.1778.
- hadronic tile calorimeter is presented as a space between two radii of 2.25 and 3.78 m filled with an iron with a stacking factor of 0.76.

As a boundary condition we use a zero value of the vector potential  $z$ -component at a circle with the radius of 13 m.

## General field behaviour

Fig. 1 displays the magnetic flux distribution over the full 8 coil toroid configuration. We plot 40 field lines which are equidistant between the vector potential minimum value of  $-1.12 V \cdot s/m$  (near the outer coil halves) and its maximum value of  $3.45 V \cdot s/m$  (near the inner coil halves). The direction of total magnetic flux density is along positive direction of the azimuth angle which is counterclockwise starting from the  $x$ -axis.

One can see that two out of 40 lines go through the outer girder tube and one additional line penetrates inside the tile calorimeter. It consists together 7.5% of magnetic flux. As was shown elsewhere [5] the values of magnetic flux density induced by toroid field inside the outer girder tube are comparable with the maximum magnetic flux density produced by the coils in the middle of each toroid sector. These values one can read from Fig. 2 where radial dependence of total magnetic flux density ( $B_t$ ) and its angle with respect to radius are shown in the second sector for three different azimuthes. The same dependences for radial ( $B_r$ ) and azimuthal ( $B_\phi$ ) magnetic flux density components are demonstrated in Fig. 3.

## Harmonic analysis of the field

To know more about the field structure we have performed the field harmonic analysis in two ways. First, we used the circles with the normalization radius of 7.23 m and with the centres placed in an origin of the Cartesian coordinate system in which we have described the general layout of the toroid magnetic system (see Fig. 1). We did the harmonic analysis using the radii of 7.23, 8.0, 8.5, and 8.9 m. The main harmonics defining the field are eighth and sixteenth. The contribution of sixteenth harmonic decreases from 24.9% to 14.4% of eighth harmonic contribution with increasing the radius from 7.23 to 8.9 m. The contribution of the dipole harmonic is 0.04% of eighth harmonic contribution at 7.23 m and decreases to 0.01% with increasing the radius. The contribution of eighth harmonic increases more than twice with the radius increasing. The contributions of other harmonics are vanished. We should note here and further that we have used only the first 20 harmonics in our analysis.

Second, we placed the circles with the normalization radius of 0.1 m in the

centre of the second sector: at the radius of 7.23 and at the azimuth of  $45^\circ$ . We did the harmonic analysis at the radii of 0.1, 0.5, 1.0, 1.5, 2.0, 2.5, and 2.8 m with respect to the sector centre. This type of the field analysis has felt only the first three harmonic terms. The contribution of the quadrupole term is 1.94% of the dipole contribution, and the contribution of the octopole term is 0.08%. Thus, we conclude that the field has almost pure dipole character in the sectors between the coils. Azimuthal dependences of total magnetic flux density and its angle with respect to radius are shown in Fig. 4.

## Reflection of the coil displacements in the field changes

To investigate an influence of the coil displacements to the field behaviour we pay our attention on the field values along radii at azimuthes of 11.25, 33.75, 45, 56.25, 78.75, and 90 degrees. Except of the basic configuration with 8 unshifted coils we calculated 5 sets of magnetic system with the first coil shifted and additional 7 sets with both first and second coils shifted.

The mnemonics using in these sets of calculations are as follows:

- **1UN** – the coil at  $22.5^\circ$  is unshifted;
- **1CL** – the coil at  $22.5^\circ$  is rotated around the centre of this coil by 5.22 mrad clockwise;
- **1CN** – the coil at  $22.5^\circ$  is rotated around the centre of this coil by 5.22 mrad counterclockwise;
- **1DP** – the coil at  $22.5^\circ$  is shifted along negative azimuth by 1 cm perpendicularly to radius;
- **1UP** – the coil at  $22.5^\circ$  is shifted along positive azimuth by 1 cm perpendicularly to radius;
- **1RO** – the coil at  $22.5^\circ$  is shifted along the radius by 1 cm outwards;
- **2RI** – the coil at  $67.5^\circ$  is shifted along the radius by 1 cm inwards;
- **2CL, 2CN, 2DP, 2UP** – are used to describe the displacements of the coil at  $67.5^\circ$  in a similar way as for the first coil.

First, we have compared the field behaviours near the second coil in dependence of the first coil displacements described above. We have subtracted the values of azimuthal component at  $56.25^\circ$  from its values at  $78.75^\circ$  and have done the same for the absolute values of radial component. The results are presented in Fig. 5. In the same way we compare the field at  $90^\circ$  and  $45^\circ$ . The results are displayed in Fig. 6.

From these figures and from more comprehensive tables we have concluded that only two sectors symmetrical around the moved coil are feeling the coil displacements. The influence of the first coil shifts to the field around the second coil is in limits of  $\pm 20$  G.

Now we concentrate on the field values along the radii at  $33.75^\circ$  and  $11.25^\circ$ . In Figs. 7–11 we plot the radial dependences of differences between the absolute values of magnetic field components at these azimuths (we subtracted the values at  $11.25^\circ$  from the values at  $33.75^\circ$ ). In the caption to each plot we mark in parenthesis the type of the first coil displacement, meanwhile the legends reflect the second coil shifts. We have to note that the bumps at the radius of 9.2 m are caused by an irregularity of the triangle mesh near transition from smaller cell size to larger cell size and should be ignored.

From these plots, in which we present the behaviour of  $B_r$ ,  $B_\phi$  and  $B_t$ , one can see that all the curves reflect well in unique way the types of the first coil displacements and are almost independent from the second coil movements. We conclude, therefore, that the coil displacements of an order of 1 cm could be register by measuring the field near each coil on its both radial sides. Such a type of measurements could be done with restricted amount of the Hall probes having well known positions with respect to the coordinate system [6]. The field does not feel the radial coil shifts (see Fig. 7), but feels well the coil rotations and its azimuthal displacements. The maximum values of the field differences shown in Fig. 8–11 reach 60–110 G.

## Conclusions

A direct reconstruction of completely inhomogeneous barrel toroid field using its measurements and Laplace equation is too hard task to be realized. Two ways out are possible. One is to measure a field in one sector and propagate these measurements to the whole toroid, neglecting the field changes caused

by small coil displacements. In the regions of large muon drift chambers an accuracy of the field knowledge will be at the level of 1% assuming the contribution due to the coil displacements to be at the level cited above. In the regions of small muon drift chambers the field knowledge can be worse.

A second way is to calculate the field, adjusting the coil positions to the field monitoring information performed with a restricted number of the Hall probes. An idea to put six  $B_r$ -measuring probes and six  $B_\phi$ -measuring probes on each coil side at the edges of the large muon drift chamber module [6] seems to be very attractive to monitor the coil displacements. Further studies are needed to show a possibility to recognize the type of coil deviations with restricted amount of probes.

*Acknowledgements.* The authors are thankful to C.W. Fabjan and W. Kozanecki for the initiation of this work and lots of prolific discussions.

## References

- [1] V.I. Klyukhin, B.I. Klochkov, *A Second Life of the CERN POISSON Program Package*. CERN Computer Newsletter 217 (1994) 18–19.
- [2] *ATLAS Technical Proposal for a General-Purpose pp Experiment at the Large Hadron Collider at CERN*. CERN/LHCC/94-43, LHCC/P 2, 15 December 1994.
- [3] W. Kozanecki, *Toroid parameters for field computations*. Memorandum of 20 July 1994.
- [4] M. Nessi et al., *Computer Models for the TILECAL Magnetic Field Distributions*. ATLAS Internal Note TILECAL-NO-012, May, 1994.
- [5] V.I. Klioukhine, B.I. Klochkov, *General behaviour of the ATLAS solenoid magnetic field calculated with the modified CERN POISSON package*. ATLAS Internal Note TILECAL-NO-022, 15 August 1994.
- [6] C. Guyot, M. Virchaux, *Transparencies shown at the Toroid Meeting held at CERN 08-09-94*. ATLAS TORO-TR-4, 20 September, 1994.

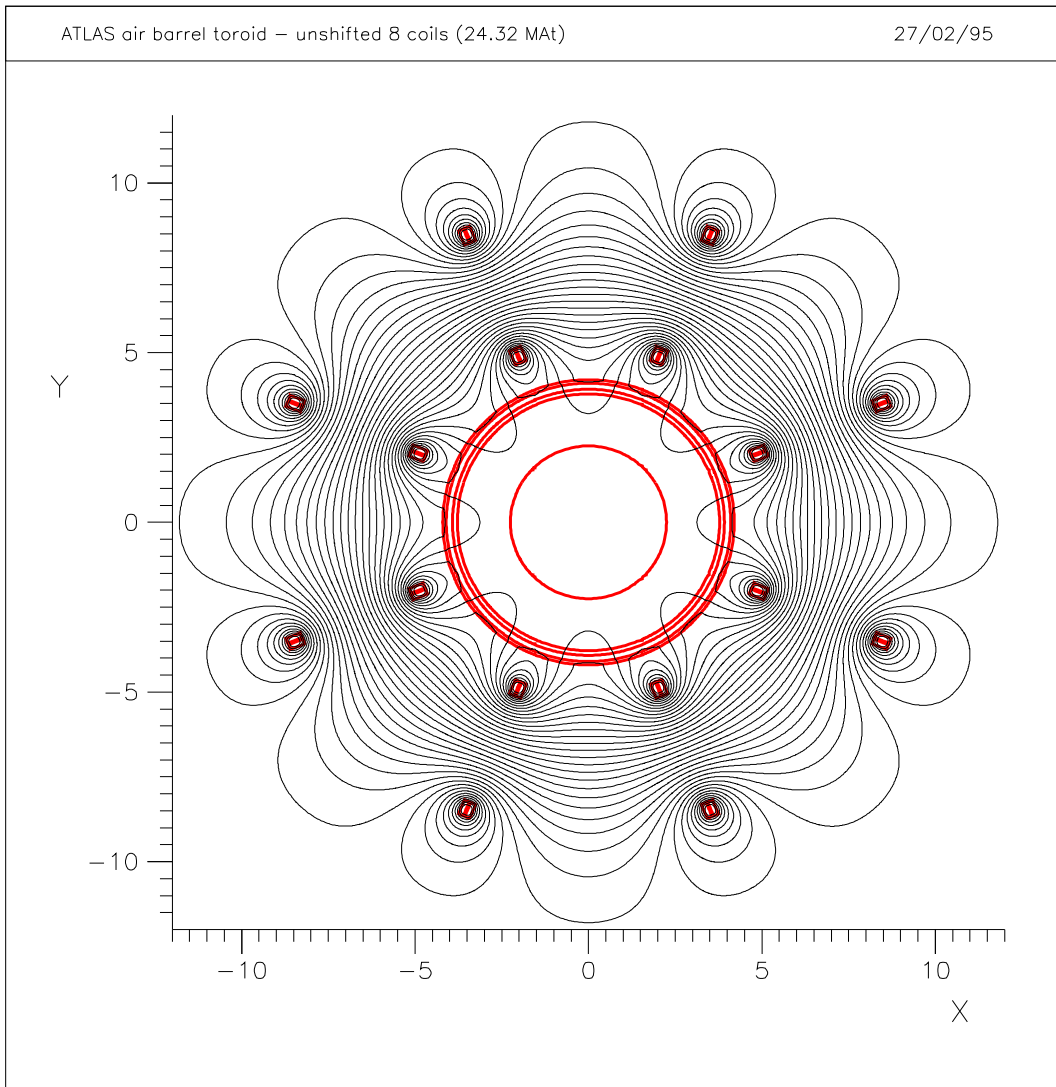


Figure 1. General layout of eight coil barrel toroid cross section.

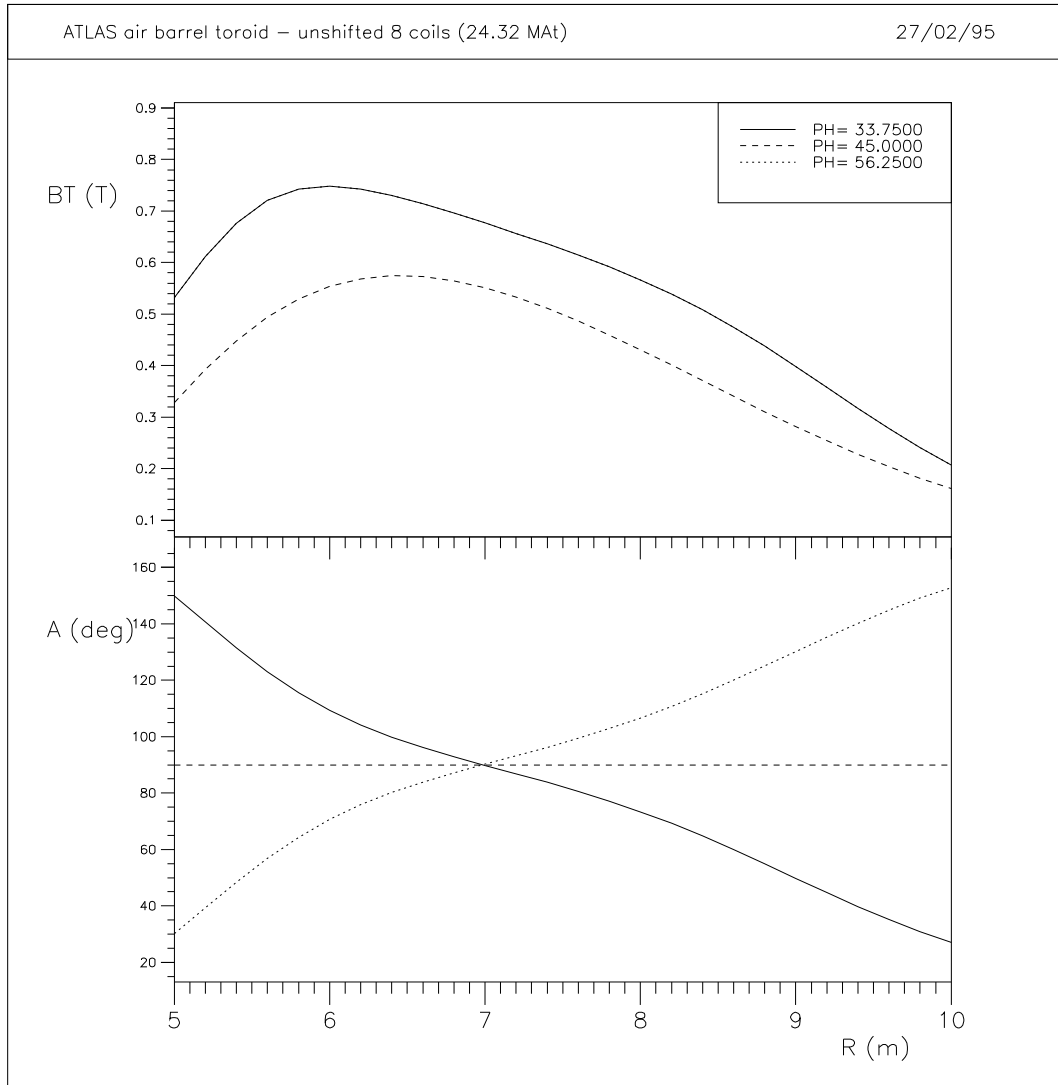


Figure 2. Radial dependences of total magnetic flux density and its angle w.r.t. radius at different azimuths.



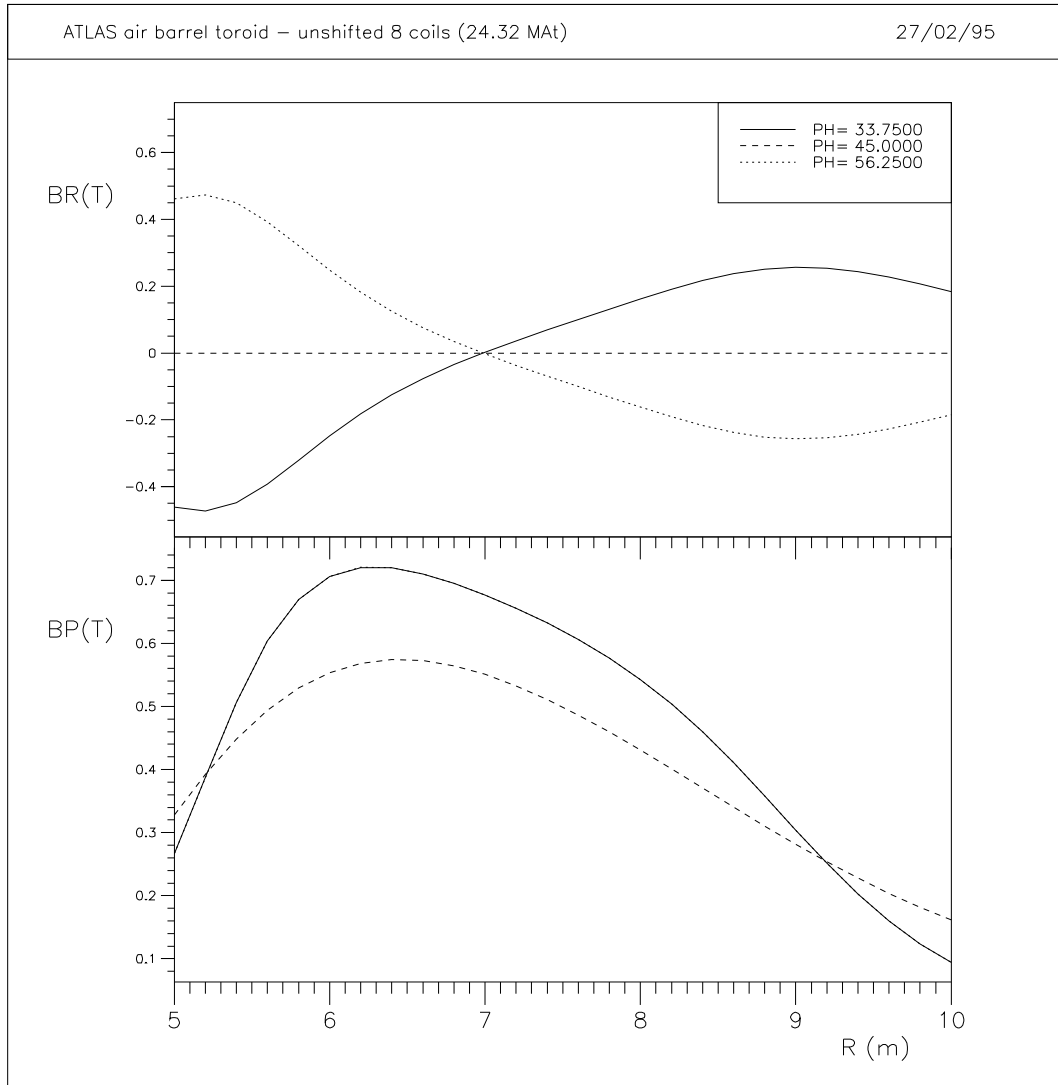


Figure 3. Radial dependences of magnetic flux density radial and azimuthal components at different azimuthes.

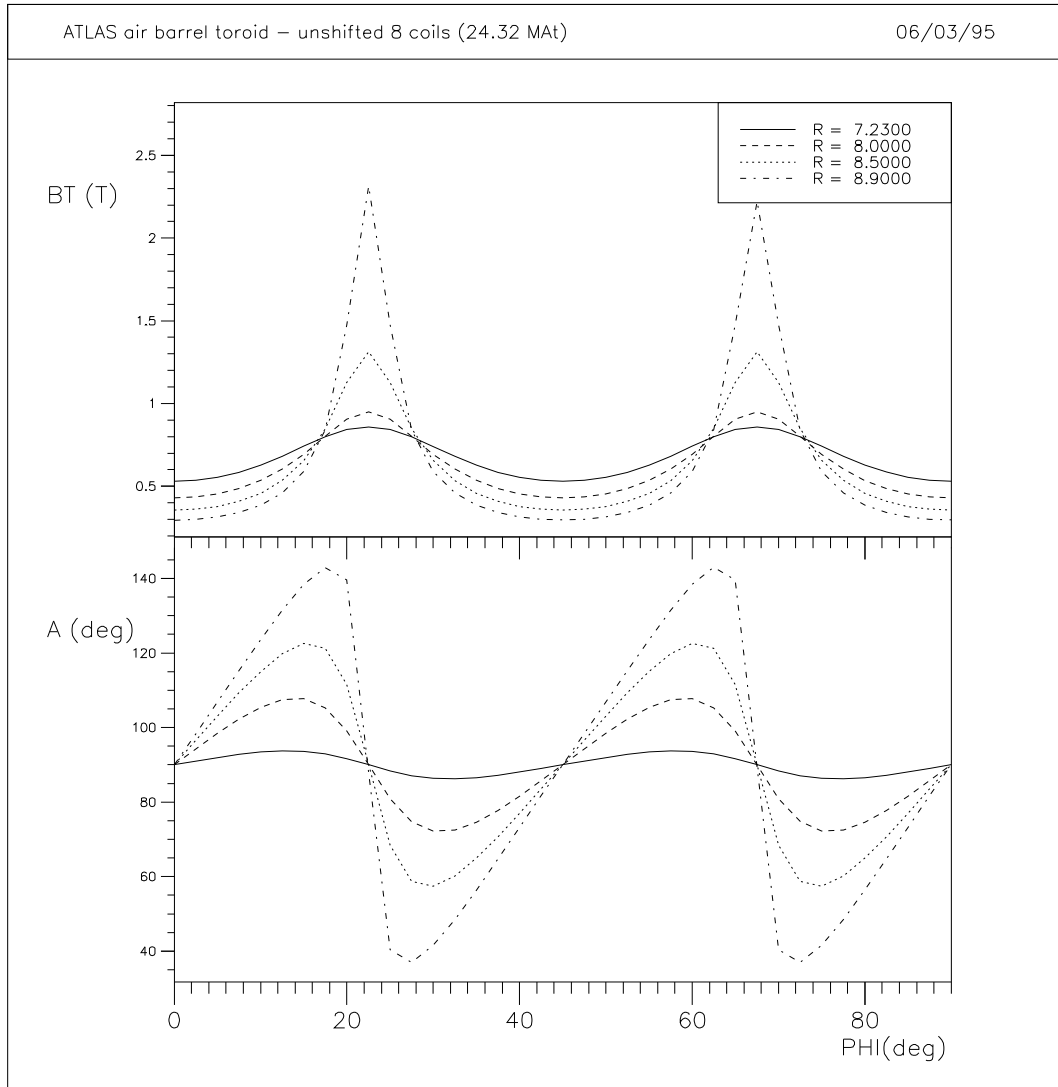


Figure 4. Azimuthal dependences of total magnetic flux density and its angle w.r.t. radius at different radii.

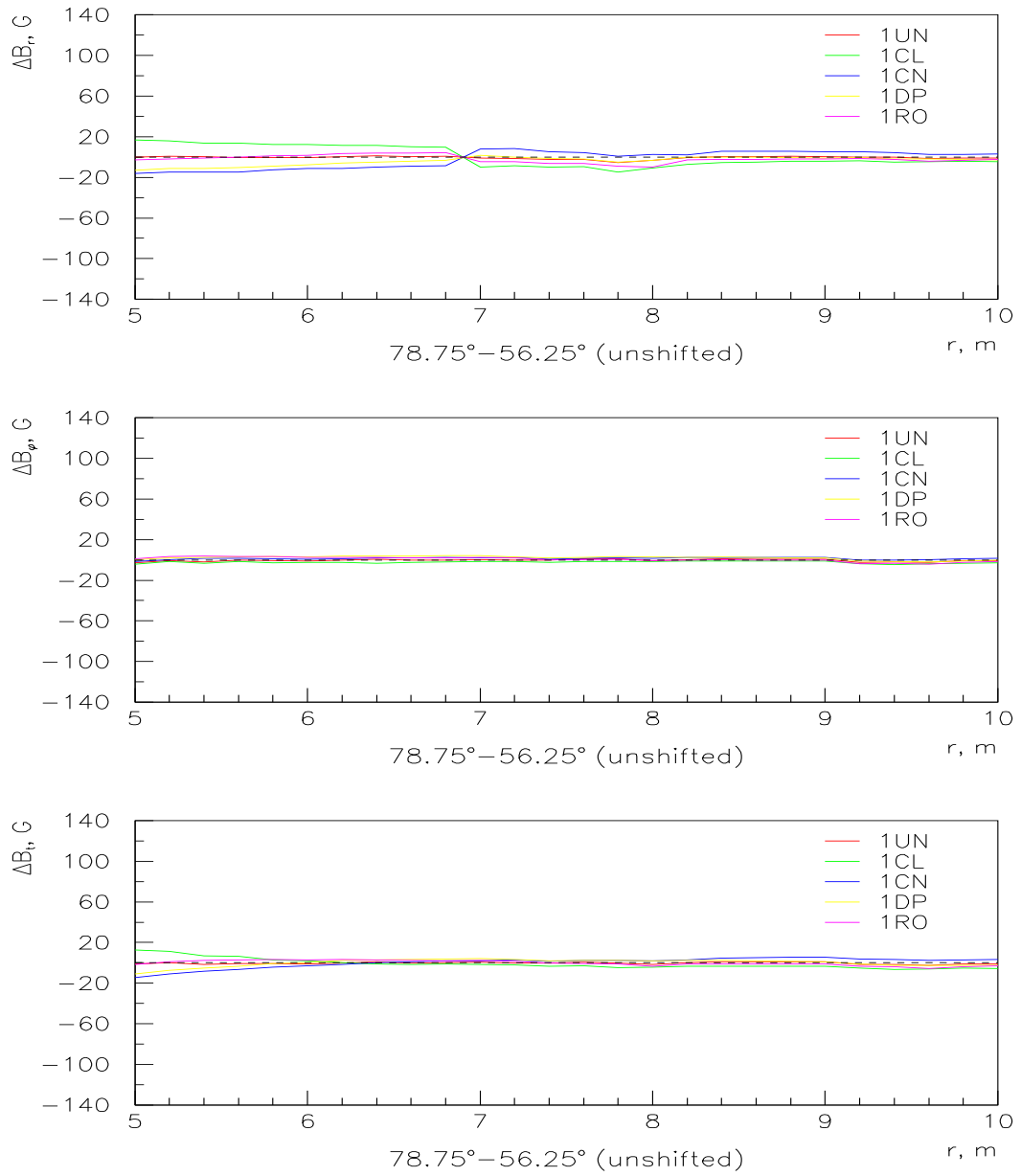


Figure 5. Comparison of field values at 78.75 and 56.25 degrees near unshifted second coil.

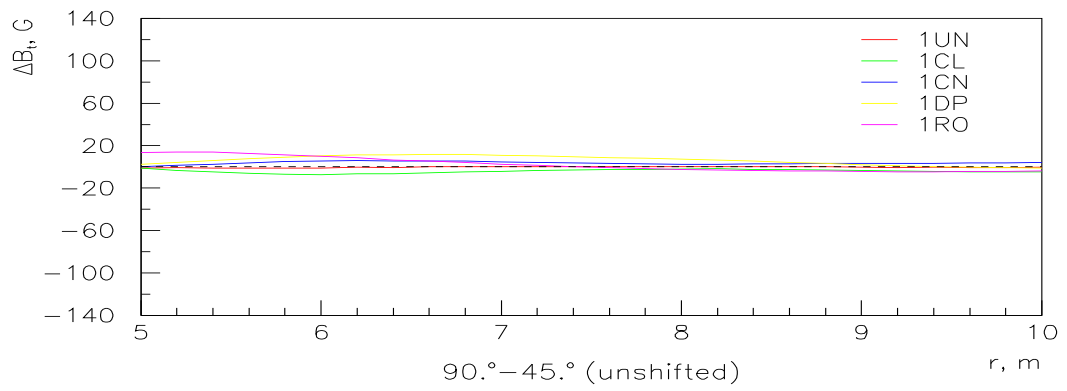
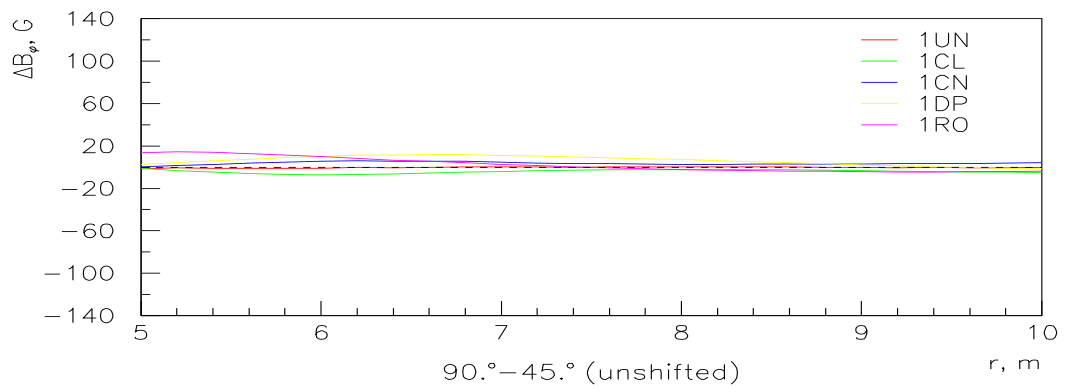
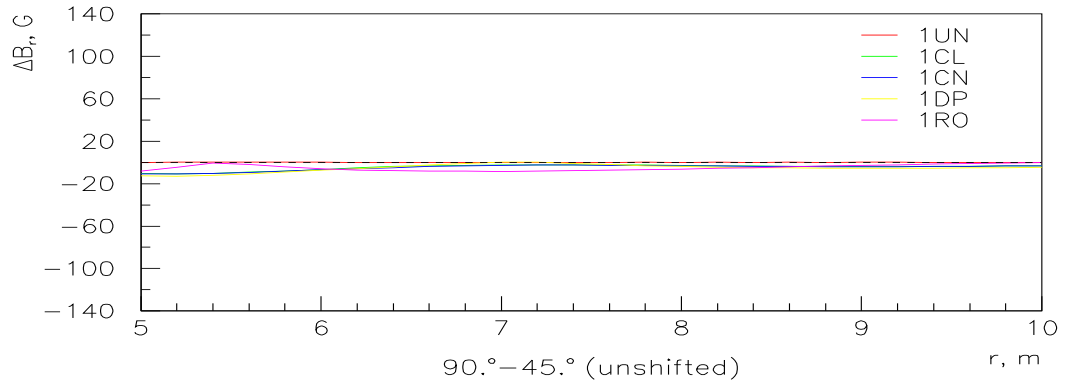


Figure 6. Comparison of field values at 90 and 45 degrees near unshifted second coil.

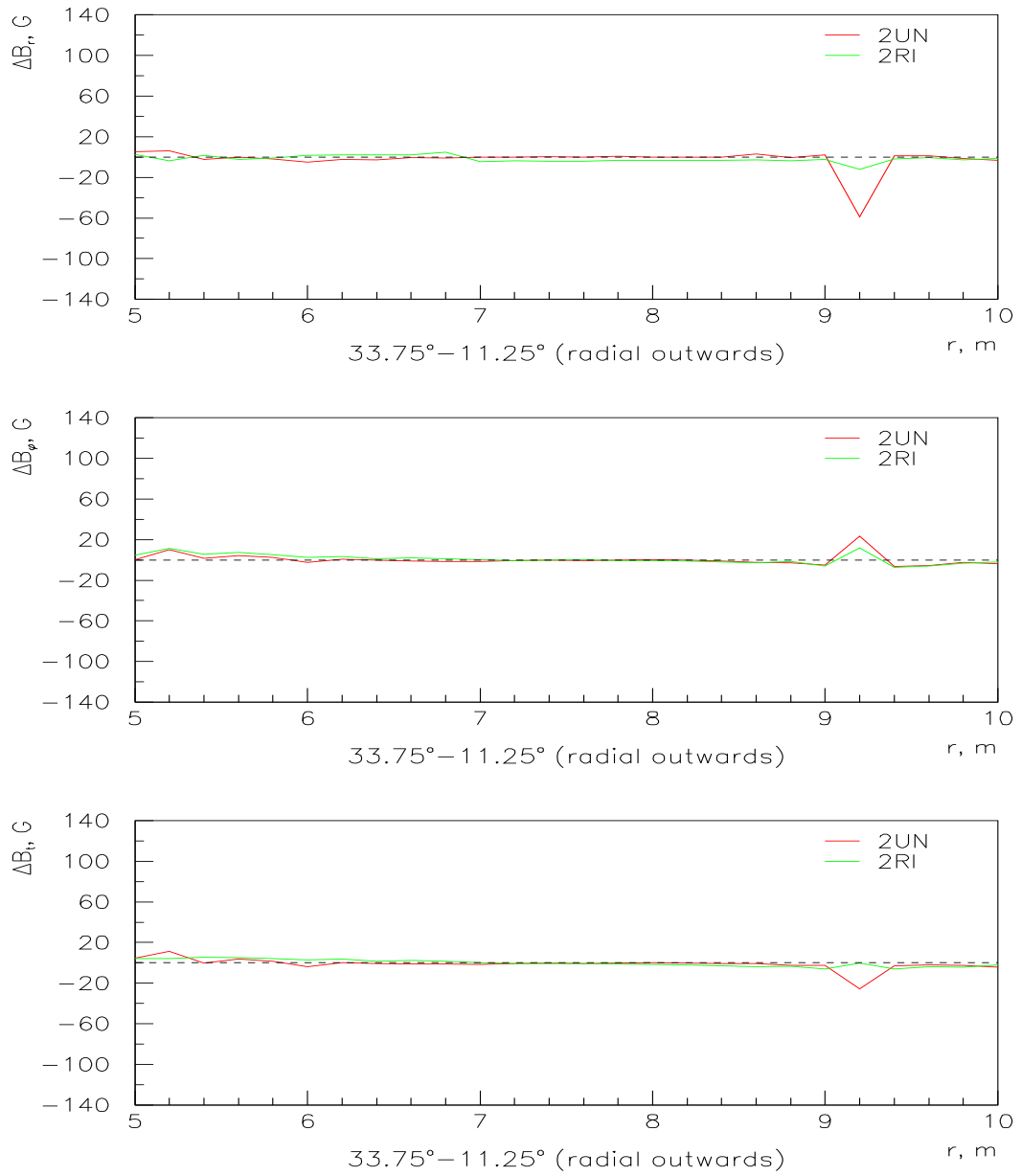


Figure 7. Comparison of field values at 33.75 and 11.25 degrees near radially shifted first coil.

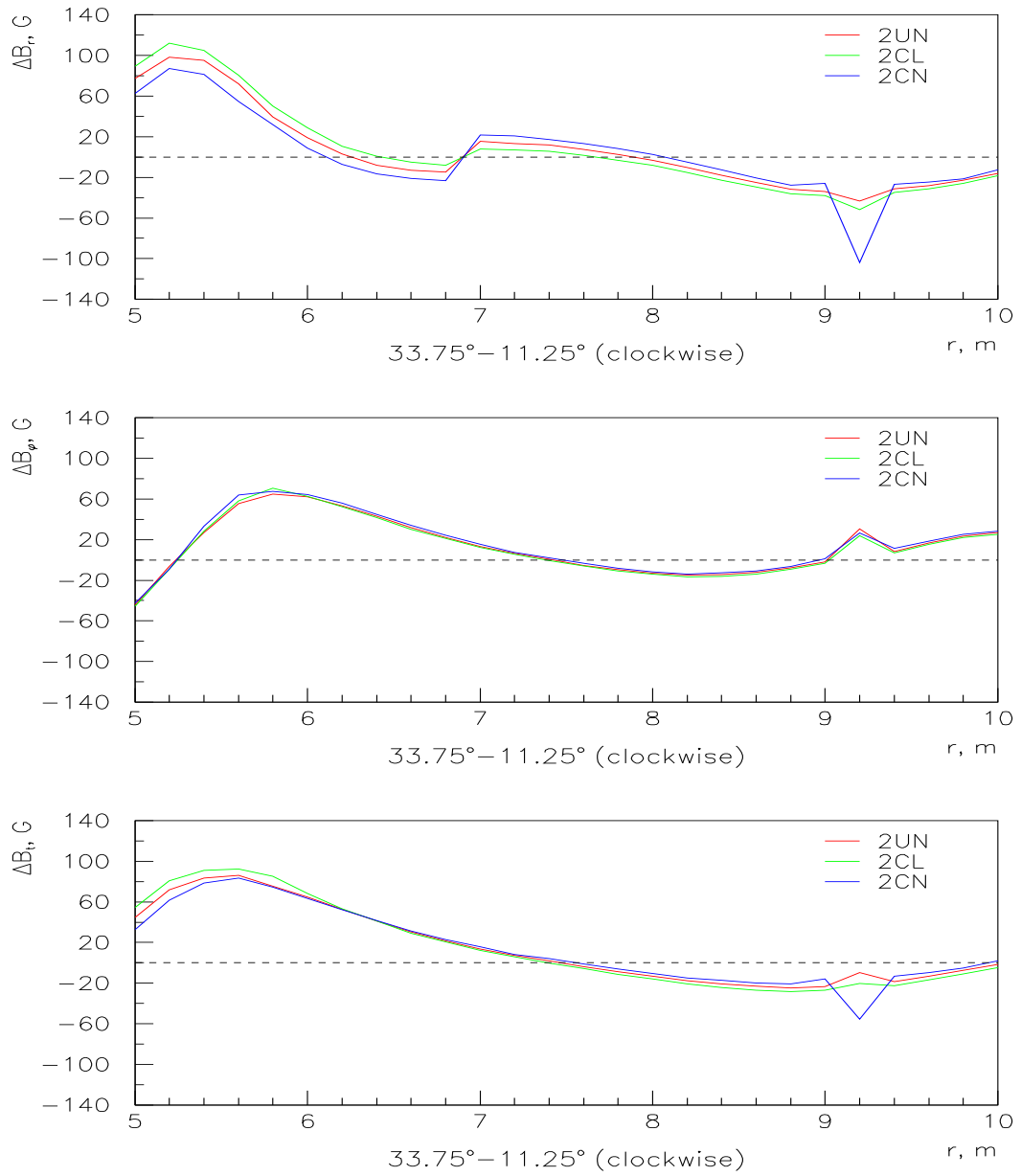


Figure 8. Comparison of field values at 33.75 and 11.25 degrees near clockwise rotated first coil.

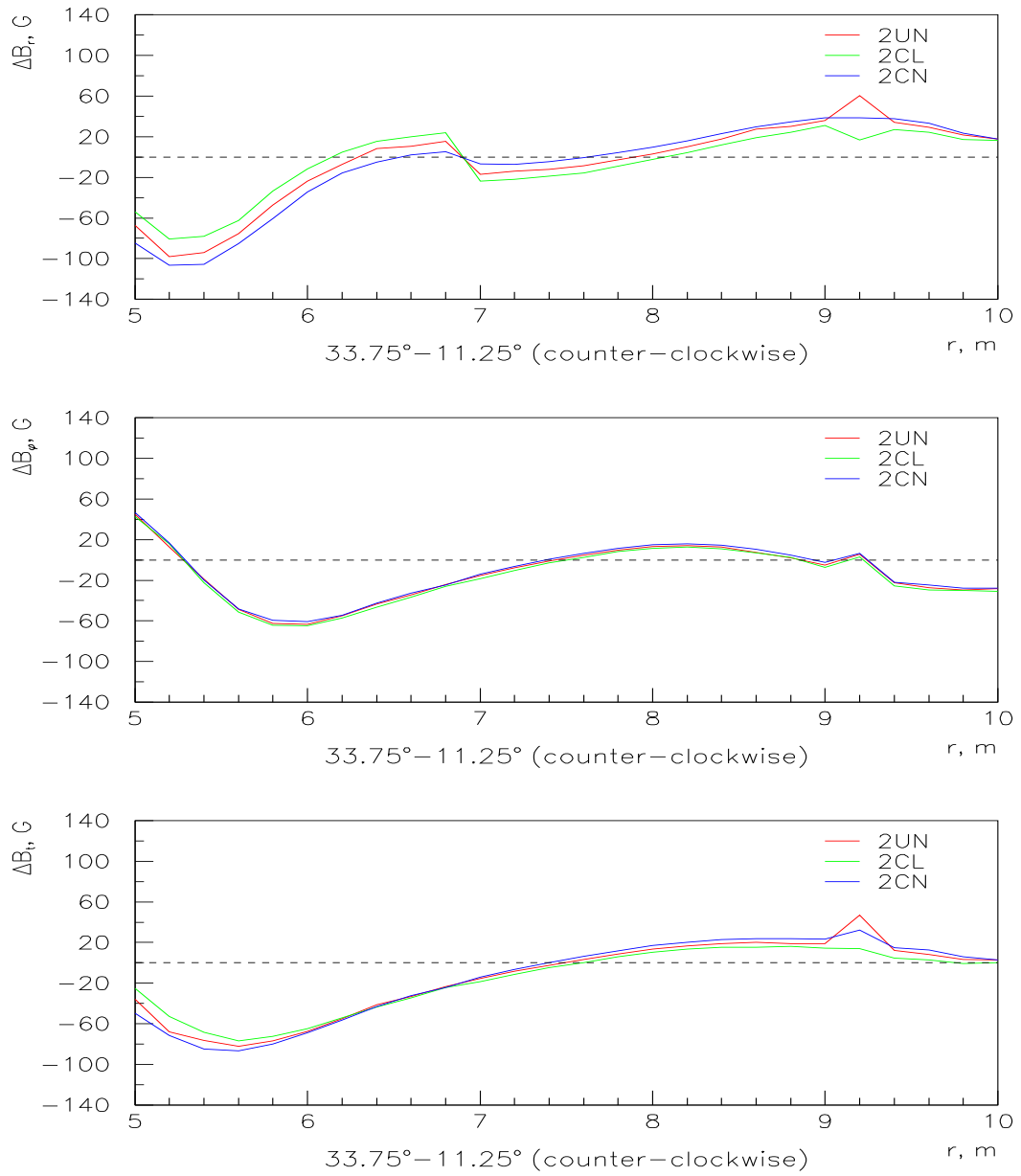


Figure 9. Comparison of field values at 33.75 and 11.25 degrees near counterclockwise rotated first coil.

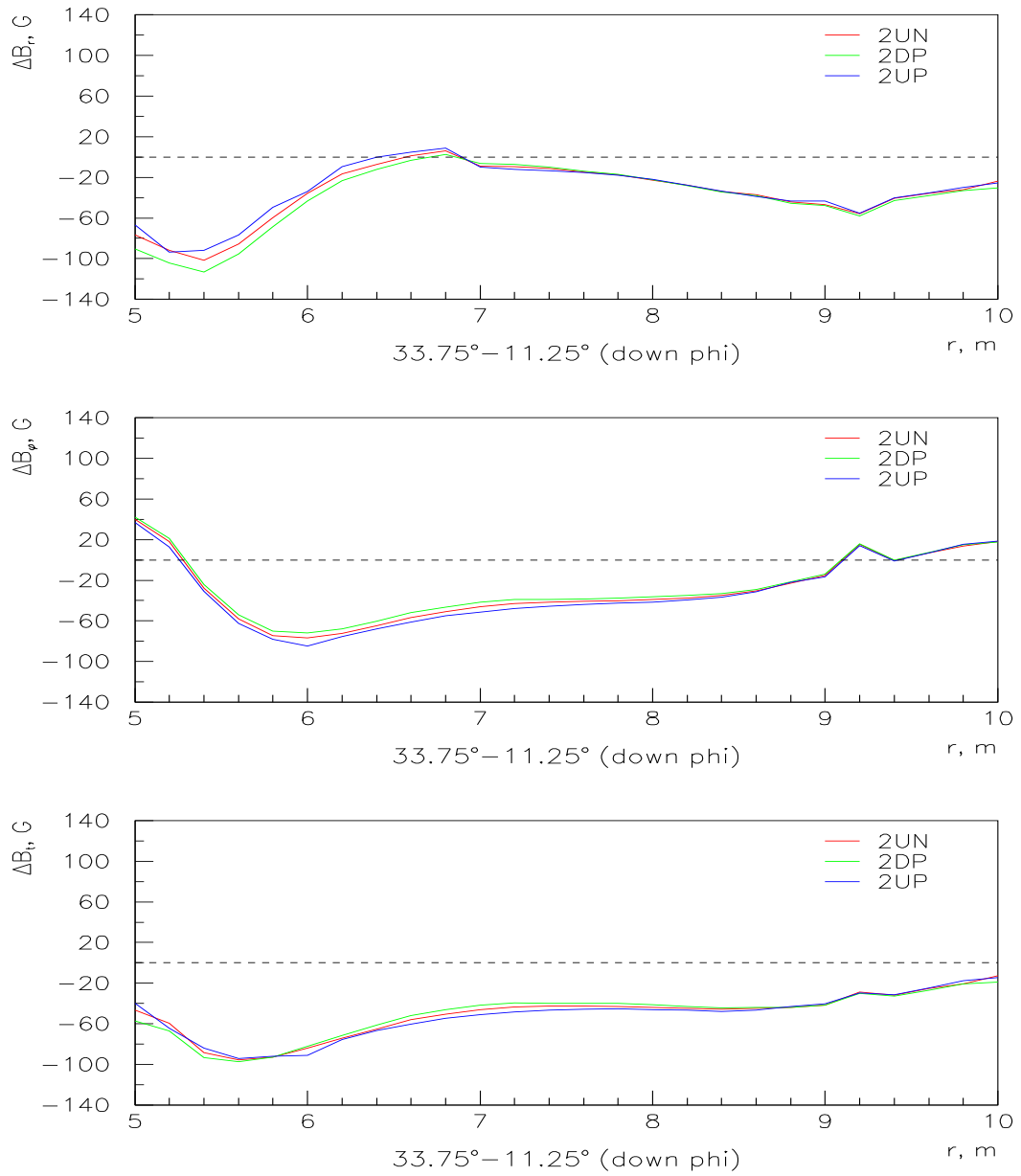


Figure 10. Comparison of field values at 33.75 and 11.25 degrees near the first coil shifted down to azimuth.



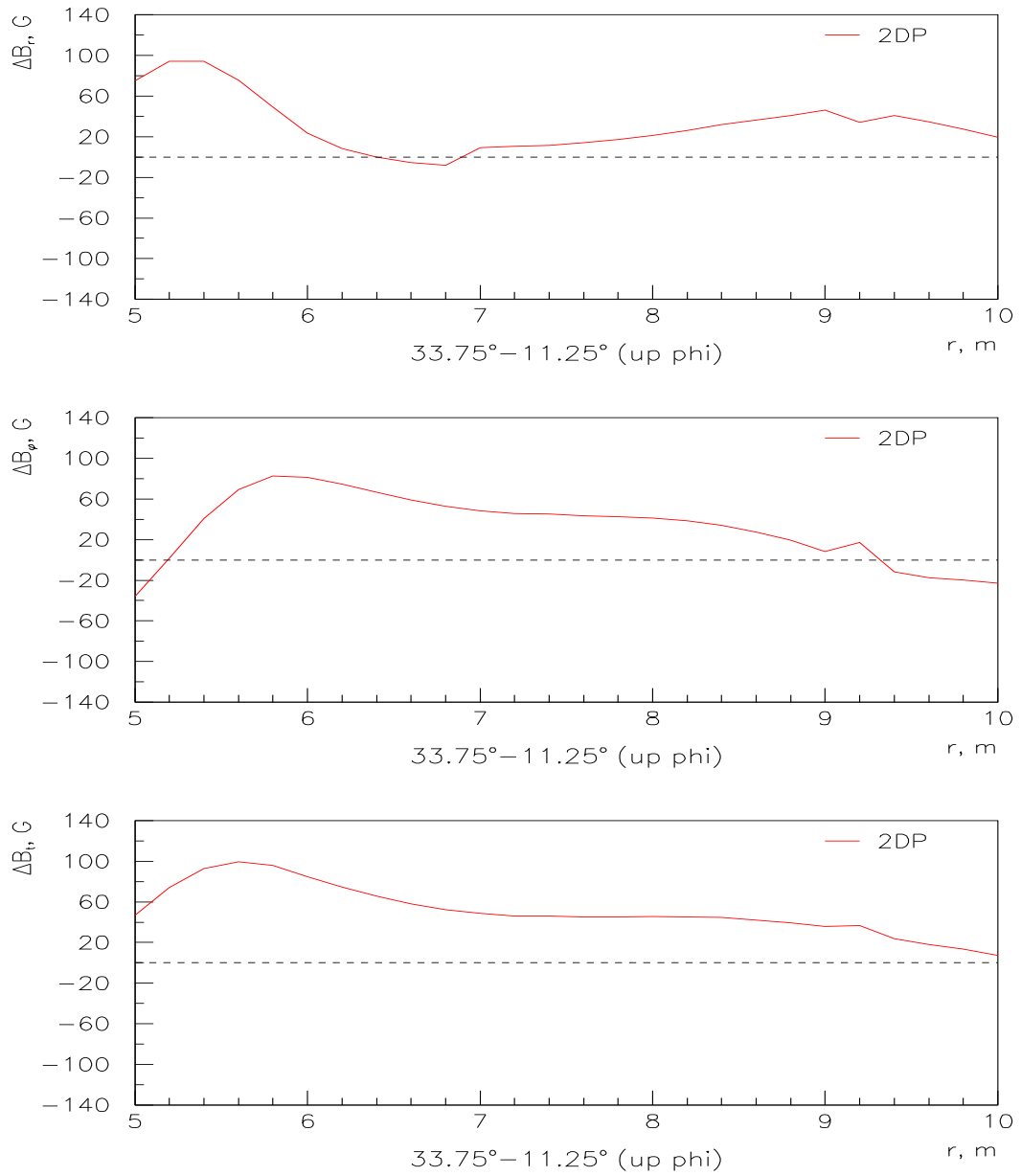


Figure 11. Comparison of field values at 33.75 and 11.25 degrees near the first coil shifted up to azimuth.